J Mater Sci (2007) 42:5340–5346
DOI 10.1007/s10853-006-0902-1

Formation of monetite nanoparticles and nanofibers in reverse micelles

Kun Wei · Chen Lai · Yingjun Wang

Received: 19 January 2006 / Accepted: 29 August 2006 / Published online: 29 March 2007

Abstract Reverse micelles solution of water and cyclohexane containing either cetyltrimethylammonium bromide (CTAB) or polyoxyethylene-8-dodecyl ether ($C_{12}E_8$) surfactants and *n*-pentanol as co-surfactant have been used as organized reaction microenvironments for monetite (dicalcium phosphate anhydrous, DCPA) precipitation. Well-crystallized monetite nanoparticles with various morphologies such as spheres, nanofibers and bundles of nanowires were obtained in CTAB reverse micelles solution. The molar ratio of water and surfactant (W_o) and the molar ratio of co-surfactant and surfactant (P_o) have great influence on the structure and morphology of the final products. A generalized mechanism for the growth of monetite in reverse micelles is proposed, in which the interaction between the surfactant molecules and PO_4^{3-} ions leads to the formation of a surfactant/$CaHPO_4$ complex. It is because of this central complex that the further fusion with reactant ions containing reverse micelles will occur only in one direction. Changing the content of water and co-surfactant has great influence on the morphology of reverse micelles and on the interaction between the surfactant/$CaHPO_4$ complex leading to a fine tuning of the morphology of products. By contrast, lacking of this interaction in the $C_{12}E_8$ system only tablet amorphous calcium phosphate can be formed.

K. Wei · C. Lai · Y. Wang
Key Laboratory of Specially Function Materials and Advanced Manufacturing Technology of Ministry of Education, South China university of Technology, Guangzhou 510640, China

C. Lai (✉)
Biomaterials Lab, College of Materials Science and Engineering, South China university of Technology, Guangzhou 510640, China
e-mail: laichen1110@hotmail.com

Introduction

Different modifications of calcium phosphates are the most important compounds in biomineralizing systems. While a high content of hydroxyapatite (HA) is detected in bones and teeth, octacalcium phosphate (OCP) is also present and act as a precursor phase for it. Moreover, dicalcium phosphate anhydrous (DCPA), also known as monetite ($CaHPO_4$), is also found in small proportion in urinary and dental stones [1, 2], and it is known to be a stable phase under more acidic conditions (pH < 4.8). Because of its fairly good biocompatibility and bioactivity, monetite is usually used as resorbable bone replacement materials [3, 4], and it is one important component of calcium phosphate cements. However, the use of calcium phosphate cements is limited to non- or low-load-bearing applications due to their poor mechanical performance as compared to bone. Fiber-like materials generally exhibit high tensile properties because of their low dislocation density. Thus fiber-like calcium phosphate compounds may be effective in improving the fracture toughness of combine biomaterials. Moreover, insertion of an implant in human body causes interaction between its surface, the body fluids and osteoblast cells (the cells that form new bone) [5]. Since these cells are sensitive to the physic-chemical properties of the internal, such as surface composition, surface energy, roughness and topography. Therefore, synthesis of biomaterials with specific size and morphology has attracted a lot of interest [6].

The morphology of single nanocrystals or colloidal microparticles can be controlled by the application of different methods like liquid crystalline [7], porous anodized aluminum oxide [8], laser-asserted catalytic growth [9], seed-mediated growth in solution [10] and reverse micelles [11]. Reverse micelles are suitable reaction media for controlling the morphology of nanoparticles because water

droplets can be seen as nanoreactors, favoring the formation of small crystallites with a sufficiently narrow size distribution [11–13]. In nonpolar solutions certain amphiphilic molecules form aggregates with their polar headgroups in the interior, leading to their description as ''reverse micelles.'' When a small amount of polar solvent—most commonly water—is added, the micelles swell, creating a new, confined liquid phase inside. Figure 1 shows a common surfactant molecule and illustrates the basic structure of an aqueous reverse micelle. Individual reverse micelles are highly dynamic structures whose components rearrange themselves over time and space through interactions or collision, coalescing and redispersing. However, reverse micelles solutions are usually thermodynamically stable mixtures of 4 components: surfactant, co-surfactant, organic solvent, and water. The co-surfactants (usually medium chain linear alcohol which involving 4–6 carbon atoms in chain) partition themselves among the oil, water, and interface domains to attain the appropriate packing of amphiphiles at the interface. As some parameters change such as surfactant concentration, temperature, salinity, content of water and co-surfactant, micelles can be deformed and can change their shapes to rod-like, hexagonal and lamellar micelles or liquid crystal. It is these changes that make it possible to prepare different shapes of nanoparticles from micelles synthesis microreactors [14]. Two parameters are very important to reverse micelles solution: the molar ratio between water and surfactant (W_o), and the molar ratio between alcohol (co-surfactant) and surfactant (P_o). Thesis parameters control the overall size of the inside water cavity, thus controlling the reactant concentrations, the position of reactants within the cavity and the size of the product particles [15, 16]. The aim of this work is to synthesize pure monetite nanomaterials with controlled morphologies for biomedical applications by using CTAB and $C_{12}E_8$ as surfactants and *n*-pentanol as co-surfactant in a reverse micelles system. The analysis of the influence of the type of surfactant and the concentration of water and co-surfactant in the solution allows to study the mechanism of formation and directional growth of the monetite nanoparticles.

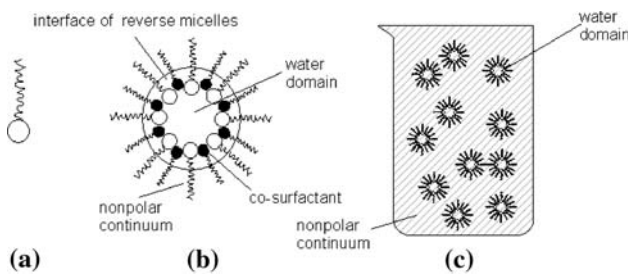

Fig. 1 Structure of (**a**) a single surfactant molecule, (**b**) a reverse micelle, (**c**) a reverse micelles solution

Materials and methods

All starting materials used in this investigation are analytical-grade. $CaCl_2$ is used as Ca source and $(NH_4)_2HPO_4$ is used as P source. The cation surfactant used in our experiments is cetyltrimethylammonium bromide (CTAB), while the co-surfactant is *n*-pentanol. Cyclohexane is used as continuous oil phase. Throughout the whole set of experiments following parameters were kept constant: 0.1 M CTAB in cyclohexane, 1 M $CaCl_2$ and 0.5 M $(NH_4)_2HPO_4$ aqueous phase solution, while the molar ratio between water and surfactant (W_o) was varied between 5 and 10 and the molar ratio between *n*-pentanol (co-surfactant) and surfactant (P_o) was 3–5. The pH value was adjusted at a constant value of 3 by ammonia addition. It should be pointed out that when W_o increases, the concentration of the reactant ions in an individual reverse micelle can be treated as constant. Because the reverse micelles will be swollen by solubilizing more water molecules, under this conditions, we can neglect the concentration fluctuation of reactant ions in the reverse micelles although the overall amount of them are increased a little with W_o value.

The Ca-containing reverse micelles solution was prepared by adding Ca^{2+} solution to the CTAB containing cyclohexane and the *n*-pentanol, and placed on the magnetic stirrer for half an hour until a transparent isotropic solution was obtained. The same procedure was repeated to prepare the P-containing reverse micelles. Then the two reverse micelles solutions were rapidly mixed, and stirred again for half an hour until the system was transparent and uniform. In the absence of surfactants, the precipitation process of monetite occurs within 12 h. In the presence of CTAB surfactant, clear and transparent solutions are obtained after an ageing process of 2 weeks at room temperature, when a white gel-like suspending precipitation appears. The products were washed three times with ethanol and ether to remove the organic components in the system and separated by centrifuging. Finally, the white sample was dried in an oven at 100 °C for 24 h.

For the purpose of comparison, monetite formation in the nonion surfactant $C_{12}E_8$ (poly(oxyethylene-8-dodecyl ether)) system was also studied, using the same procedure described above.

The as-synthesized powders were dispersed in ethanol and their morphologies characterized by transmission electron microscopy (TEM PHILIPS CM300), using an accelerating voltage of 300 KV. Energy diffractive X-ray analysis (EDX) was used to obtain the element composi-

tions of the samples. The phase composition and crystallinity of powders were analyzed by X-ray diffraction (XRD) using a Bruker Diffractometer (AXS, D8 Advance) with CuK_α radiation at 40 KV and 40 mA. Fourier transform infrared absorption spectra (FTIR) were obtained by using a Nicolet Nexus spectrometer.

Results and discussion

At low water content, i.e. $W_o = 5$, small irregular spherical particles with 50 nm diameter are observed by TEM as shown in Fig. 2a. The electron diffraction pattern (in the insert) confirms that each particle is a well crystallized single crystal XRD patterns of the nanoparticles consist of narrow peaks with d spacing consistent with well-ordered crystalline monetite (Fig. 2b). The diffraction pattern can be indexed using the triclinic structure with $a = 6.9$, $b = 6.65$, $c = 7$ and space group P 1 (PCPDS-PDF: 77-0128). When more water is added to the system and W_o is enhanced to 10, fibers with more than 500 nm length and 50–100 nm diameter are obtained (Fig. 3a). The fibers have straight edges, uniform widths, and rather well-defined round ends, coexisting with some irregular tablets. The XRD patterns acquired from these randomly oriented nanofibers demonstrate that pure and well crystalline $CaHPO_4$ is the only phase present. Keeping constant the water content of the solution at a high value of $W_o = 10$, and increasing the co-surfactant/surfactant molar ratio results in great morphological changes. For $P_o = 10$, fiber bundles of 100 nm width are formed consisting of several

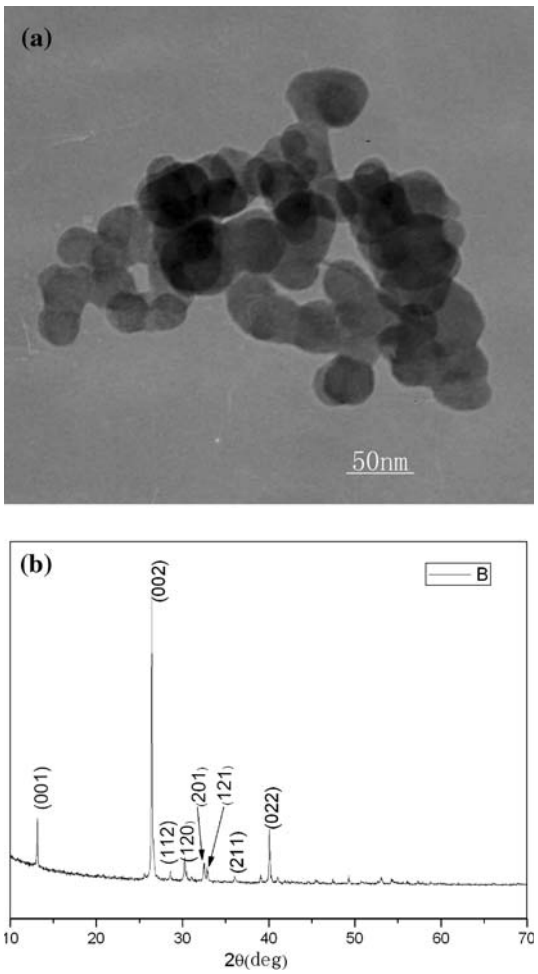

Fig. 2 Monetite nanoparticle formation in CTAB/water/cyclohexane/pentanol reverse micelles solution with low amount of water and *n*-pentanol ($W_o = 5$, $P_o = 3$). (**a**) TEM image (the insert shows the electron diffraction pattern) and (**b**) XRD spectrum of as-prepared particles

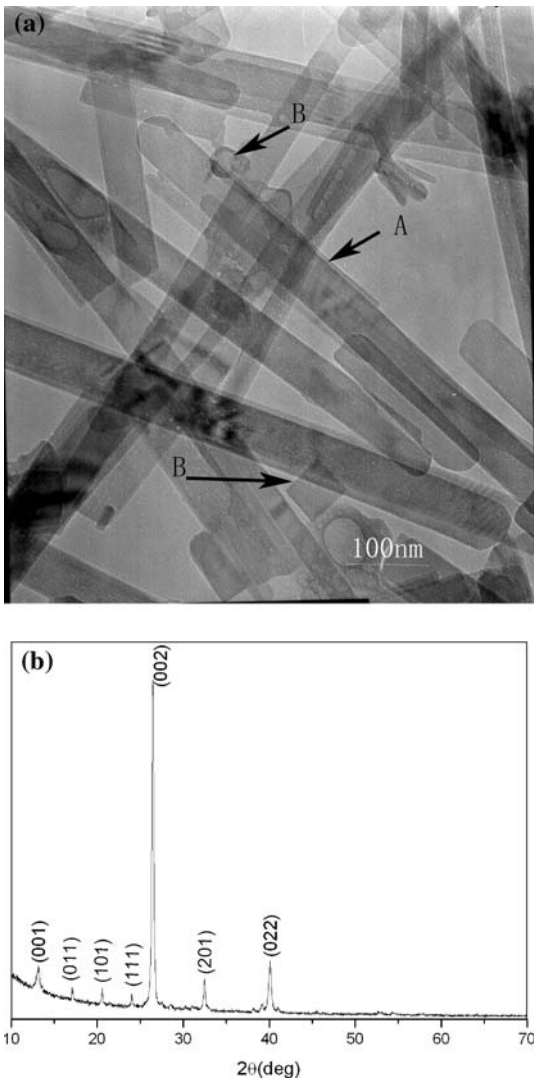

Fig. 3 Monetite nanofibers formation in CTAB/water/cyclohexane/pentanol reverse micelles solution with higher water content ($W_o = 10$, $P_o = 3$). (**a**) TEM (A: corresponding to the nanofibers, B: corresponding to irregular tablets), (**b**) XRD spectrum of as-prepared particles

loosely parallel filaments (Fig. 4a). Each individual filament has a uniform typical width of 50 nm along its entire length of more than 700 nm, thus forming rather nanowires. The XRD patterns of these nanowires (Fig. 4b) show no other crystalline phase than $CaHPO_4$. In contrast, when the reaction takes place in the nonion surfactant $C_{12}E_8$ reverse micelles solution, the particles are tabular in shape (Fig. 5a). Elemental analysis shows (Fig. 5b) that the material consists of Ca, P and a small quantity of Cl coming from the reactant $CaCl_2$. The atomic ratio of Ca and P in this calcium phosphate compound is 1.2. Because Ca^{2+} ions are selectively ejected during electron irradiation so that the measured Ca:P ratios can be lower than nominal (1.28) [17]. The small peak beside the main Ca peak is the subpeak of Ca. No distinctive peak is observed in the XRD patterns (Fig. 5c) indicating that the calcium phosphate compound formed in this nonion surfactant system is amorphous.

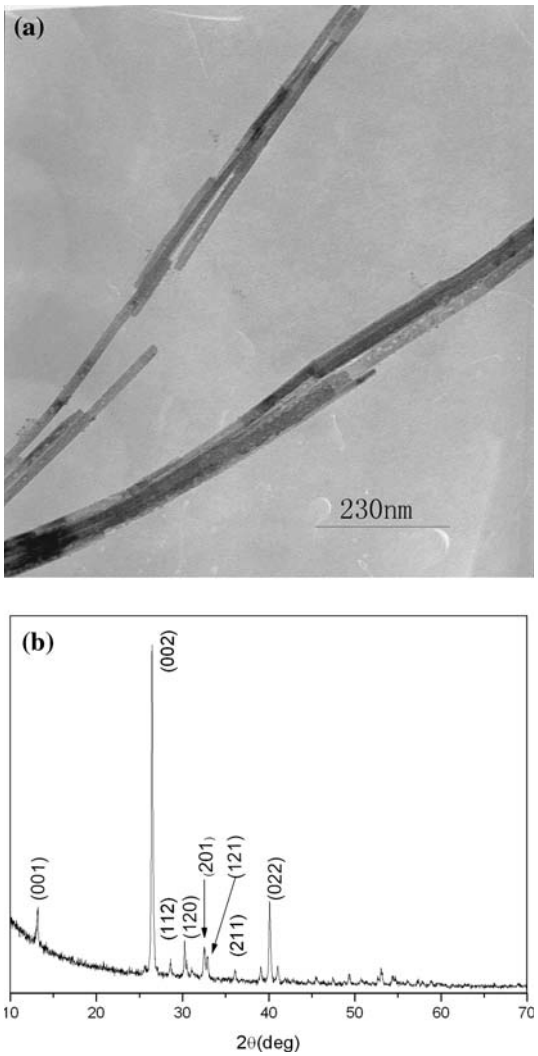

Fig. 4 Monetite nanowire bundles formed in CTAB/water/cyclohexane/pentanol reverse micelles at higher *n*-pentanol content (W_o = 10, P_o = 10). (**a**) TEM image of monetite nanowire bundles, (**b**) XRD spectrum of as-prepared particles

A more thorough examination of the XRD patterns of the spherical nanoparticles, nanofibers and bundles of nanowires directs some noteworthy intensity changes observed. For (001) and (hkl) diffraction lines in such a manner that several of them as (112), (120) and (211) disappear in the XRD pattern of nanofibers. This can be seen from the patterns recorder for 2θ values range from 26 to 40 (Figs. 2b, 3b, 4b). On the other hand, the peaks of (011), (101) and (111), which can not been observed in XRD patterns of spherical nanoparticles and nanowires bundles, appear in the nanofibers XRD pattern. According to this, the relative variation in the intensities of the (002) and (022) diffraction lines observed in all three XRD patterns, can be tentatively considered as an approximation for measuring the corresponding variation in the z/y growth direction ratio of the various nanoparticles. As result, the z/y corresponding to the spherical particle, nanofibers and nanowires bundles are 5.13, 6.28, and 4.02, respectively, showing that the peak intensity of the (002) peak versus the intensity (022) peak for the nanofibers in Fig. 3b is higher than the intensity ratio of the others. Generally, higher intensity of groups of peaks in powder XRD is a feature crystallite grains. These results indicate that nanofibers prefer growing along *c* axis.

The results reveal that the precipitation of calcium phosphate compounds in reverse micelles solution can be markedly influenced by the nature of the surfactant and the supermolecular architecture of the self-assembling aggregates. In the cation surfactant reverse micelles solution, the cation surfactant CTAB ionizes completely in water phase leading to formation of positive amino headgroups with tetrahedral structure [18]. With the addition of the phosphate reactant, PO_4^{3-} ions which are also tetrahedral structure may bound to one or more headgroups at the interface of the micelles (as shown in Fig. 6b) by electrostatic interaction and structure complementarity. In the reverse micelles solution, the effects of Brownian motion lead to fusion–fission between reverse micelles, thereby the reactants are exchanged, mixed, and react to form the products [19]. When two reverse micelles involving different reactant ions collide in solution, they are fused by mutual association forming $CaHPO_4$ nuclei. In addition, further fusion processes with other Ca^{2+}-containing and PO_4^{3-}-containing reverse micelles will occur as depicted in Fig. 6. When the amount of water and co-surfactant are lower (W_o = 5, P_o = 3), the reverse micelles are so small that the charge density in them is so high that the fluidity in the interfacial zone is reduced [18]. Thus, under these conditions the reverse micelles in the solution can be considered as small and rather rigid spheres, limiting spatially the

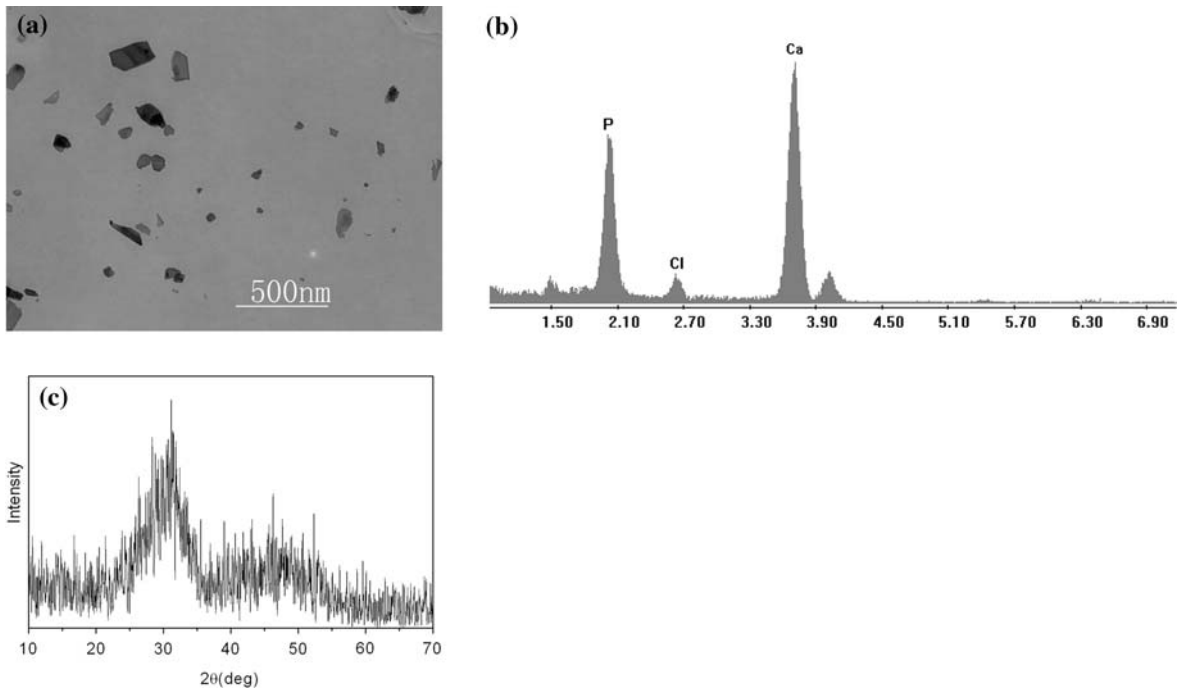

Fig. 5 Monetite formation in $C_{12}E_8$/water/cyclohexane/pentanol reverse micelles, $W_o = 10$, $P_o = 3$. (**a**) TEM image of monetite tabular nanoparticles, (**b**) EDX spectrum of as-prepared particles, (**c**) XRD spectrum of as-prepared particles

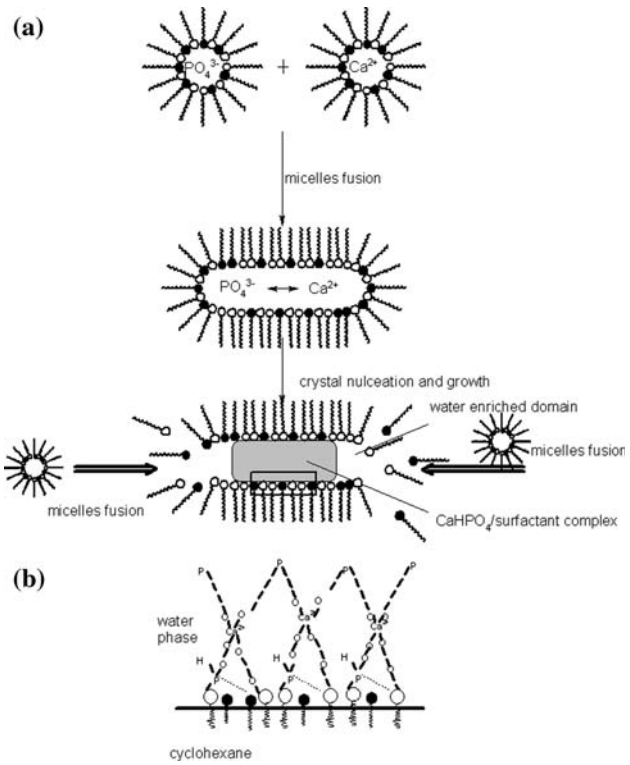

Fig. 6 (**a**) Illustration in the formation of monetite nanoparticles formed in CTAB/water/*n*-pentanol/water/cyclohexane reverse micelles solution. (**b**) Enlarged illustration for the interaction between the crystal and the surfactant molecule at the inner side interface

crystal growth. This could account for the formation of the small spherical nanoparticles obtained in Fig. 2a. At higher water content ($W_o = 10$), the long fibers with rather well-defined round ends were obtained in our experiment which can be observed in Fig. 3a. Although Brownian motion effects make the reverse micelles unstable and frangible, the formation of so larger and well-crystallized particles suggest that reverse micelles must have provided static growth conditions for the nanofibers in our experiment. A rational assumption is now that in our experiments the fusion of reverse micelles is irreversible, that is to say, reverse micelles will not be fissile after fusion. It is because of the association between CTA^+ and PO_4^{3-} that the fusion process of reverse micelles in our experiment is irreversible. As suggested above, a general mechanism of development of nanofibers is proposed. At the beginning, the intense stir favors the formation of smaller reverse micelles. When the stir stopped, the Ca^{2+}-containing and PO_4^{3-}-containing reverse micelles collide and fuse together as amorphous nuclei. Because of the strong affinity for ionized amino group of CTAB mentioned above, PO_4^{3-} ion are immobilized by the CTA^+ at the water and oil interface, and the reaction with Ca^{2+} ions therefore occurs in close proximity to the interface (as shown in Fig. 6b), which leads to the formation of the complex of ''amorphous nuclei ($CaHPO_4$)/surfactant.'' This is the reason why no deposition could be observed immediately in our experiment when the Ca^{2+}-containing solution and PO_4^{3-}-containing solution were

mixed. Figure 6b illustrates the combination of amorphous nuclear and surfactant molecules. As for the CTAB reverse micelles several researchers [20] have shown that they form wormlike aggregations in solution. Under this conditions, the worm-like reverse micelles are composed of a centrally located amorphous $CaHPO_4$/surfactant complex with water-enriched domains at the two ends of the shaped aggregates (shown in Fig. 6a). Dynamic exchange with other reveres micelles would then be significantly faster at these two ends of the fusion pair than in the central region containing the nucleated cluster because surfactant molecules in the water enrich domain can dissociate into the oil phase to exchange with the isolated surfactant molecules in oil phase [21]. In contrast, the surfactant molecules associated with the central located $CaHPO_4$ complex (the gray rounded rectangle shown in Fig. 6a) would be immobile because of strong interaction between PO_4^- and CTA^+ (Fig. 6b). The uni-directional fusion of reverse micelles provides the possibility for crystal growing along one direction and would be responsible for the long nanowires observed in Fig. 3a. In general, linear growth could represent the lowest energy configuration that couples the requirements for particle–particle fusion (reduction in surface free energy and increase in bulk lattice energy) and minimization of membrane curvature (sphere to cylinder transformation) [22]. However, here were still many small tablets coexisting with the nanofibers. On one hand, in acid solution tablet form is the preferred crystal habit of $CaHPO_4$ [23]. One the other hand, for many template phases consisting of surfactant molecules, as the mineral nucleate and grows large enough, it is necessary to expel some surfactant molecules from the volume occupied by the mineral, and it is possible for a surfactant molecule to diffuse away from the growing mineral without ever exposing its hydrophobic or hydrophilic segments to domains of opposite nature [24]. As such there are still a small amount of crystals would assume their most favorable configuration. The same phenomenon which the shape mismatch between inorganic structures and the template has also been observed in other researchers' experiments [7, 24]. In context with previous observations confirms that the interaction between the surfactant molecules and $CaHPO_4$ nuclear are not tight for all time, and it will diminish gradually with the growth of crystal.

Addition of short chain Alcohols are known to reduce the rigidity of the water-in-oil interface of reverse micelles and are generally considered responsible for increasing their fusion [25], thus allowing enhanced exchange of solubilized matter and, consequently, Ostwald ripening. The loading of *n*-pentanol into the interface of the micelles corresponds to the increase in the total interface with a corresponding decrease of the interfacial film thickness [26]. In our experiments, *n*-pentanol partitions strongly into the interfacial film reducing the surfactant molecules density per area at the micellar interface, and the interaction between the crystal and the surfactant molecules will be weakened by increasing of the *n*-pentanol concentration. Moreover, the shape fluctuation of the reverse micelles will also be favored. Thus providing possibilities for the formation of nanoparticles with larger size and morphological diversity. When the rigidity of the micellar interface is reduced, their coalescence may take place in any direction instead of only along their ends. The individual droplets slowly self-assemble and fuse along the side faces of the nanofibers by interdigitation of the organic chains [21] as shown in Fig. 7. Such an effect could account for the formation of the coherently aligned nanofibers which are shown in Fig. 4a

By comparison, nonion surfactant $C_{12}E_8$ is almost nonionized in water phase, thus the interaction between PO_4^{3-} and the polyether headgroups of $C_{12}E_8$ reverse micelles will be weaker than with CTAB, resulting in homogenous nucleation in the water cavity. Without the growth guiding effect of the surfactant molecules, calcium phosphate develops assuming their most favorable configuration and the coalescence of reverse micelles takes place in any direction. Losing the strong affinity between CTAB surfactant molecules and amorphous $CaHPO_4$ nanoparticles, reverse micelles in this system will exchange more rapidly, leading to unstable conditions not favorable for the transformation from the amorphous nucleus to larger crystals. Thus, formation of the amorphous calcium phosphate gel in this nonion surfactant system undergoes a similar growth process as in the aqueous solution or in a water-alcohol medium without surfactant [27].

Conclusion

Different morphologies DCPA nanoparticles have been prepared by varying the surfactant and co-surfactant concentration in a reverse micelles solution. In CTAB surfactant system, at low water and co-surfactant content ($W_o = 5$, $P_o = 3$), small irregular spherical particles with 50 nm diameter can be obtain. When more water is added to the system and W_o is enhanced to 10, fibers with more than 500 nm length and 50–100 nm diameter are obtained. Keeping constant the water content of the solution at a high value of $W_o = 10$, and increasing the co-surfactant/surfactant molar ratio to $P_o = 10$, fiber bundles of 100 nm width are formed and consisted of several loosely parallel filaments. Each individual filament has a uniform typical width of 50 nm along its entire length of more than 700 nm, thus forming rather nanowires. XRD patterns show that the main phase is well-crystallized $CaHPO_4$. In contrast, products prepared in $C_{12}E_8$ the particles are

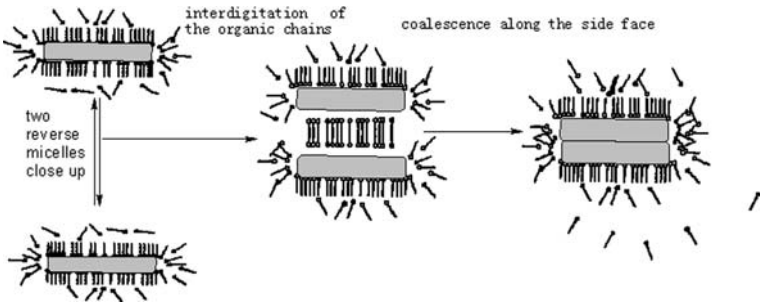

Fig. 7 The sketch of the fusion along the side face of reverse micelles1

tabular in shape. Elemental analysis and XRD patterns show that the material is amorphous calcium phosphate compounds.

Based on the resulting morphology of long and straight nanofibers it is possible to expect that the fusion process of micelles are irreversible and unidirectional. So the aggregation and coalescence of individual droplets determine the growth direction of the crystal. A strong association between the $CaHPO_4$ and surfactant molecules throughout the development of the crystal could be responsible for the apparent stability of the $CaHPO_4$/surfactant complex, causing the formation of well-crystallized monetite and long nanofibers morphology. Lacking this kind of interaction, nonion surfactant $C_{12}E_8$ has negligible influence on the shape of the crystal, and the formation of monetite under this condition is comparable to that in water. Varying water content in reverse micelles leads to the shape changes in reverse micelles, causing the structural evolution of crystal. Addition of alcohol results in reduction of the interaction of crystal and surfactant molecules and increasing the fluidity of the reverse micelles interface leading to the fact that reverse micelles coalescence can take place in many directions. By interdigitation of the organic chains, reverse micelles fuse along the side faces of nanofibers. Such effect may have accounted for the formation of nanowires bundles.

Our findings demonstrate that the shape of the material produced is related to the condition of microreactors. The shape of nanomaterials can be fine tuned by varying the parameters of reaction system. The production of nanofibers, tablets and nanowires bundles in our experiments represents a useful route to the biomineralization of inorganic structures with complex form.

Acknowledgements The authors acknowledge the financial supports for this study from National Natural Science Foundation of China (NSFC) Project Grant (50272021, 59932050, and 50472054), Natural Science Foundation Cooperative Project Grant of Guangdong (04205786). We also thank Dr. B. Léon for her helpful comments and suggestions.

References

1. Daudon M, Donsimoni R, Hennequin C, Fellahi S, Le MG, Paris M, Troupel S, Lacour B (1995) Urol Res 23:319
2. Werness PG, Bergert JH, Smith LH (1982) J Cryst Growth 53:166
3. DeGroot K (1983) Bioceramics of calcium phosphate. Florida CRC Press, Boca Raton
4. Williams DF, (1985) Biocompatibility of tissue analogs, vol 11. Florida CRC Press, Boca Ration
5. Shwartz Z, Lohmann CH, Oefinger J, Bonewald LF, Dean DD, Boyan BD (1999) Adv Dent Res 13:38
6. Andrés-Vergés M, Fernández-Gpmzález C, MartÍnez-Gallego M (1998) J Euro Ceram Soc 18:1245
7. Huang LM, Wang HT, Wang ZB, Mitra AP, Zhao DY, Yan YS (2002) Chem Mater 14:876
8. Yin AJ, Li J, Jian W, Bennett AJ, Xu JM (2001) Appl Phys Lett 79:1039
9. Duan X, Lieber XM (2000) Adv Mater 12:298
10. Jana NR, Gearheart L, Murphy CJ (2001) Adv Mater 13:1389
11. Sui XM, Chu Y, Xing SX, Yu M, Liu CZ (2004) Mater Lett 58:1255
12. Hirai T, Asada Y, Komasawa I (2004) J Colloid Interf Sci 276:339
13. Uskokovic V, Drofenik M, Ban I (2004) J Magn Magn Mater 284:294
14. Liu Y, Zhang Z (2002) In: Wang ZL (ed) Handbook of nanophase and nanostructured materials-synthesis. Tsinghua University Press, Bei Jing, p 9
15. Pileni MP (1993) J Phys Chem 97:6961
16. Clark S, Fletcher PDI, Ye X (1990) Langmuir 6:301
17. Senger B, Brès EF, Hutchison JL, Voegel JC, Frank RM (1992) Philos Mag A 65:665
18. Y Li, Li YD, Deng ZX, Zhuang J, Sun XM (2001) Inter J Inorg Mater 3:633
19. Faeder J, Ladanyi BM (2000) J Phys Chem B 104:1033
20. Törnblom M, Henriksson U (1997) J Phys Chem B 101:6028
21. Hopwood JD, Mann S (1997) Chem Mater 9:1819
22. Li M, Mann S (2000) Langmuir 16:7088
23. Jinawath S., Polchai D., Yoshimura M (2002) Mater Sci Eng C 22:35
24. Braun PV, Stupp SI (1999) Mater Res Bull 34:463
25. Curri ML, Agostinao A, Manna L, Monica MD, Catalano M, Chiavarone L, Spangnolo V, Lugará M (2000) J Phys Chem B 104:8391
26. Palazzo G, Lopez F, Giustini M, Colafemmina G, Ceglie A (2003) J Phys Chem B 107:1924
27. Sarda S, Heughebaert M, Lebugle A (1999) Chem Mater 11:2722